Influence of apparatus geometry and deposition conditions on the structure and topography of thick sputtered coatings

John A. Thornton

Telic Corporation, 1631 Colorado Avenue, Santa Monica, California 90404

Two cylindrically symmetric and complementary sputtering geometries, the post and hollow cathodes, were used to deposit thick ($\sim$25-μ) coatings of various metals (Mo, Cr, Ti, Fe, Cu, and Al-alloy) onto glass and metallic substrates at deposition rates of 1000–2000 Å/min under various conditions of substrate temperature, argon pressure, and plasma bombardment. Coating surface topographies and fracture cross sections were examined by scanning electron microscopy. Polished cross sections were examined metallographically. Crystallographic orientations were determined by x-ray diffraction. Microstructures were generally consistent with the three-zone model proposed by Movchan and Demchishin [Fiz. Metal. Metalloved. **28**, 653 (1969)]. Three differences were noted: (1) at low argon pressures a broad zone 1–zone 2 transition zone consisting of densely packed fibrous grains was identified; (2) zone 2 columnar grains tended to be faceted at elevated temperatures, although facets were often replaced by smooth flat surfaces at higher temperatures; (3) zone 3 equiaxed grains were generally not observed at the deposition conditions investigated. Hollow cathode deposition accentuated those features of coating growth that relate to intergrain shading.

INTRODUCTION

The structure of thick vacuum-deposited coatings is determined by a sequence of morphological changes which occur as the coating grows in thickness from discrete initial nuclei, and by grain boundary migration and recrystallization which may occur concurrently.[1] Thus, in addition to the relevant grain boundary energies, the growth process is dependent on the incident coating flux, the coating atom adsorption probabilities, the density of surface sites, and the adatom surface mobility. These parameters depend in turn on the coating atom energy and angle of incidence, the exposed crystallographic surfaces, the presence of foreign atoms, and most important, the substrate temperature. As in bulk grain growth and recrystallization studies, one expects useful correlations in terms of T/T_m, where T is the substrate temperature and T_m is the coating material melting point (K). After examining thick coatings of Ni, Ti, W, Al_2O_3, and ZrO_2, Movchan and Demchishin[2] (M & D) divided the T/T_m scale into three zones: zone 1 ($T/T_m < 0.25$–0.3), consisting of tapered crystallites with domed tops which increase in width with temperature; zone 2 (0.25–$0.3 < T/T_m < 0.45$), consisting of columnar grains with smooth matt surface; and zone 3 ($T/T_m > 0.45$), consisting of equiaxed grains and bright surface. Similar zones have been suggested by Sanders.[3] There is considerable evidence of evaporated coating structures that support the M & D model.[4–7]

Little work has been reported on structure of thick sputtered coatings.[8–11] Sputter deposition involves several factors that make it different from evaporation: (1) sputtered atoms have considerable kinetic energy (an average of 4–40 eV); (2) energetic sputtered atoms may simultaneously approach substrate in several directions; (3) ambient gas is always present; and (4) substrate may be subjected to plasma bombardment.

This paper reports on the structure of relatively thick ($\sim$25-μ) coatings of various metals that were dc sputter-deposited under various conditions of T/T_m, argon pressure, and plasma bombardment, using two cylindrically symmetric and complementary sputtering geometries, the post and hollow cathode (see Table I).

PREPARATION OF COATINGS

Three experimental arrangements were used: (1) hollow cathode with fixed-temperature substrate holder; (2) hollow cathode with substrate holder capable of maintaining temperature gradient (see Fig. 1); and (3) post cathode surrounded by substrate holders maintained at various temperatures.

Axial magnetic fields protected the substrates from primary-electron bombardment in both geometries. Substrates in hollow cathode were electrically isolated and floated at -30 to -50 V relative to the anode. At a typical deposition rate of 1500 Å/min the substrate heat load, due primarily to the kinetic energy and heat of condensation of coating atoms and plasma

TABLE I. Summary of experimental conditions

Coating material	Cathode type	Substrate Temperature (°C)[a]	Ar. pressure (μ)	Deposition rate (Å/min)	Substrate material[b]
Copper	Hollow	LN₂ to 500	1 to 30	100 to 3000	Glass and S.S.
Copper	Post	20 to 800	1 to 30	800 to 20 000	Glass and Ta
Al Alloy (type 6061)	Hollow	LN₂ to 500	1 to 30	1000 to 1500	Glass
Al Alloy (type 6061)	Post	LN₂ to 500	1 to 30	1000 to 2500	Glass
Titanium	Hollow	LN₂ to 1200	1 to 30	25 to 1000	Glass and Ta
Titanium	Post	20 to 1200	1	1000	Glass and Ta
Molybdenum	Post	400 to 1100	2	1000	Ta
Chromium	Hollow	LN₂	1	650	Glass and S.S.
Iron	Hollow	LN₂	1	650	Glass and S.S.

[a]LN₂ is the temperature obtained on substrate clipped to holder through which liquid nitrogen was continually flushed. Actual temperature on substrate surface was not determined.
[b] S.S. to stand for stainless steel.

radiation, was about 10^{-1} W/cm². (The ion component of ambipolar diffusion flux was about 0.3 mA/cm².)

Post cathodes were typically 3-cm o.d. by 30-cm long with substrates located at radii of 10–12 cm. Virtually no plasma species reached the substrates, which floated at a fraction of a volt relative to the anode. The substrate heat load was about 10^{-1} W/cm² at a deposition rate of 2000 Å/min. Substrate plasma bombardment was achieved in post cathode apparatus by reducing the magnetic field strength so that the plasma extended to the substrates.

The cathodes (targets) were water cooled. Aluminum alloy targets were formed from commercial 6061 tubing, copper targets from OFHC tubing, and titanium targets from commercially pure tubing. The molybdenum target was a pressed and sintered tube. Iron and chromium targets were electroplated onto stainless steel mandrels.

Substrates were 0.060-in. glass microscope slides, 0.03-in. stainless steel sheet, and 0.005-in. tantalum foil. Substrate temperatures of greater than 600°C were obtained by heating tantalum foil clamped between copper electrodes, and measured by a radiation thermometer in the hollow cathode and by chromel-alumel thermocouples in the post experiments. Temperatures of 100–600°C were obtained by clamping substrates onto stainless steel holders containing nichrome heaters and iron-constantan thermocouples. Substrate temperatures of approximately 20 and −196°C were obtained by flushing water or liquid nitrogen through copper or aluminum substrate holders.

The apparatuses were evacuated to between 5×10^{-7} and 10^{-6} Torr with 4-in. oil diffusion pumps prior to deposition. Under these conditions, the residual gas flux was a factor of about 10^{-5}–10^{-6} smaller than the typical sputtered flux. Argon (99.998%) was used as working gas. Deposition conditions are summarized in Table I. Hollow cathode discharge voltages were in range 500-800 V, post cathodes in range 700-1000 V.

EXPERIMENTAL RESULTS

Coating surface topographies and tensile-fracture cross sections were examined by scanning electron microscopy. Cross sections of coatings that could not be fractured were polished and examined metallographically. Sample SEM micrographs are shown in Figs. 2 and 3. The dependence of gross structural
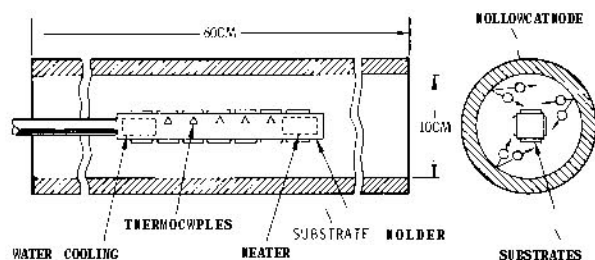

FIG. 1. Schematic of hollow cathode sputtering apparatus with temperature gradient substrate holder.
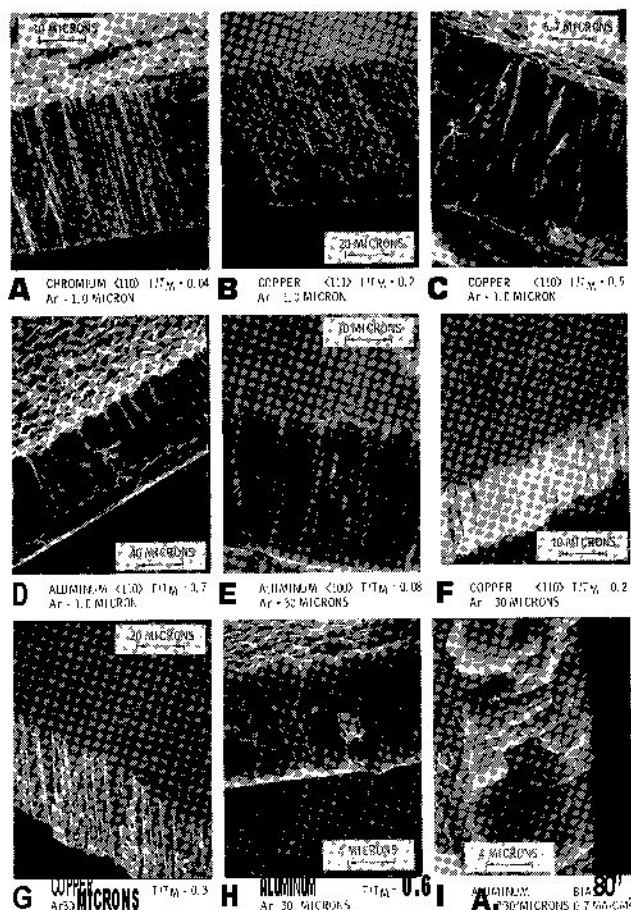

FIG. 2. Fracture cross sections of coatings deposited in hollow cathode at various substrate temperatures and argon pressures.
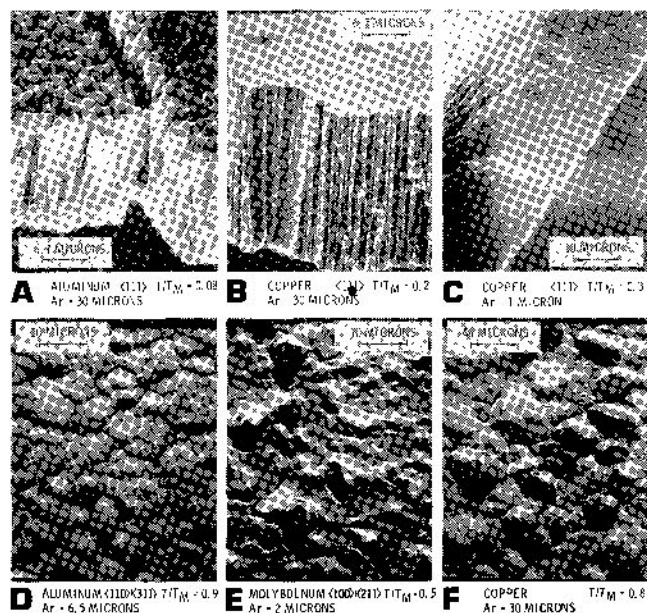
FIG. 3. Surface view and fracture cross sections of coatings deposited with post cathode at various substrate temperatures and argon pressures.

features on T/T_m and argon pressure is summarized in Fig. 4. Figure 4 was constructed primarily from Cu and Al-alloy data obtained at deposition rates of from 1000 to 2000 Å/min, but is consistent with considerable additional data obtained with Mo, Cr, Fe, and Ti. The basic features were essentially independent of the substrate material and deposition rate (for the range 1000–2000 Å/min). (Variations in the extent of the structural regions were observed for significantly higher and lower deposition rates. These influences will be reported in a future communication.)

Structural zones can be identified, consistent with M & D. At very low T/T_m, coatings exhibited a dark gray surface and consisted of tapered crystallites separated by voids, similar to M & D's zone 1 (see Figs. 2A, E, and 3A). The tendency of this structure to persist to higher values of T/T_m increased with argon pressure and was greatest in hollow cathodes (compare Figs. 2F and 3B). This structure was not observed with post cathodes at low argon pressures. In hollow cathode at high argon pressure, where voids were more exaggerated, a crystallite width-to-length increase with increasing T/T_m, identical to the zone 1 character described by M & D, was apparent (compare Figs. 2E and F).

At higher T/T_m the intergrain voids began to fill in (compare Figs. 2F and G); and the structure passed into a transition zone of tightly packed fibrous grains, which generally did not extend through the coating thickness (Figs. 2B and 3C), increased in both width and length with T/T_m, and exhibited a relatively smooth "fine-domed" surface. This transition zone covered a relatively large range of T/T_m and at low argon pressures was the dominant low temperature structure, particularly in the post cathode geometry. This region terminated at T/T_m in the range 0.3–0.5

with a zone consisting of columnar grains which extended through the coating thickness, increased in width with T/T_m (see Figs. 2C and D), and generally exhibited faceted surfaces, particularly in the hollow cathode case. This structure is very similar to the zone 2 structure described by M & D. The gross features of the columnar structure were independent of argon pressure (compare Figs. 2D and H). Coatings deposited at the low T/T_m end of the transition zone tended to be brittle. The ductility increased with T/T_m, and coatings with the zone 2-type columnar structure tended toward bulk strength and ductility. Cu and Al-alloy coatings with fine grained transition zone structures yielded tensile strengths of 20 000–75 000 psi and 60 000–75 000 psi, respectively. (Other investigators have reported high strengths for fine-grained W, Ni, and Ti coatings and a trend toward bulk properties for high T/T_m columnar structures.[2,5,6]

The columnar structure tended to persist in most of the sputtered coatings to the highest T/T_m values examined, although equiaxed grains did form in copper coatings deposited at high deposition rates (10 000–20 000 Å/min). However, at high T/T_m (~0.75) a distinct surface structure consisting of smooth flat grains with grooved boundaries was consistently observed, even on the columnar Mo, Ti, Cu, and Al-alloy coatings (Fig. 3D). Figure 3E shows a Mo coating in the transition range where a few faceted grains remain. Similar structures are seen at higher argon pressures, as shown by Cu coating in Fig. 3F. (This particular coating, deposited at 10 000 Å/min, exhibited an equiaxed structure.)

It has been shown that relatively high-energy ($\geqslant$ 500 eV) ion bombardment can suppress the formation of a distinct columnar structure in Cr,[8,12] Ta,[13] and Be.[14] Figure 21 shows coating deposited under conditions of Fig. 2F but with ion bombardment flux equal to about 80% of the coating atom flux. Distinct Al columnar structure is significantly densified even at low (80 V) ion energies.

The crystallographic orientations of about twenty-five representative coatings were examined by x-ray diffraction. All exhibited texture. At low argon pressures and T/T_m, fcc Cu and Al-alloy coatings deposited
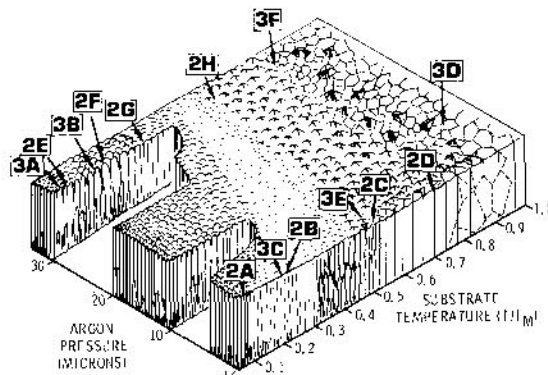

FIG. 4. Schematic representation of dependence of coating structure on substrate temperature and argon pressure.

on glass and stainless steel substrates in both the post and hollow cathodes had a <111> preferred orientation, while bcc Cr and Mo deposited under similar conditions had a <110> orientation. These observations imply a preference for orientations that place the most densely populated atomic planes parallel to the substrate. Such orientations are commonly seen in evaporated thin films[15-19] and have been reported for thick-sputtered coatings.[8,9,20] An increase in T/T_m at low argon pressures caused Cu and Al-alloy coatings deposited with both the post and hollow cathodes to assume a <110> orientation. Minor <311> orientations were consistently observed with the post cathode. Elevated argon pressures in the hollow cathodes caused Cu to assume a <110> and Al-alloy to assume a <100> orientation. (Similar observations have been reported by others.[15,21]) However, Cu and Al-alloy coatings deposited at high argon pressures with post cathode had <111> orientation at all T/T_m.

Polymorphic Ti coatings deposited on liquid-nitrogen-cooled glass substrates were in bcc ß-phase with <110> orientation. Those deposited on 20°C glass substrates were in hcp α-phase with high degree of basal plane orientation. Ti deposited on Ta substrates in the temperature range 900-1200°C consisted of a p-phase with substrate orientation and random α-phase, which was probably a transformed β-structure.[5] A thick interface diffusion zone developed at high substrate temperatures, probably as consequence of the fact that β-Ti and Ta form a continuous series of solid solutions.

DISCUSSION

At T/T, <0.1 there is little adatom surface mobility, and initial nuclei tend to grow in the direction of available coating flux.[3] The growth morphology is affected significantly by intergrain shading. Tapered crystallites develop. Intergrain boundaries are voids rather than true grain boundaries, so that coatings have poor lateral strength and are underdense, although individual crystallites have near bulk density. At high argon pressures, adsorbed argon limits the adatom mobility and permits this structure to persist to higher T/T_m. (There is evidence that residual gas adsorption can cause mobility variations over exposed crystallite surfaces.[22-24]) Hollow cathode deposition is characterized by a large side flux as shown schematically in Fig. 1, and these devices are more vulnerable than post cathodes to argon pressure effects because of intercrystallite shading and the possibility that adsorbed argon can accumulate in crevices that are protected from coating atom impact. The trend toward formation of voided structures at high argon pressures was found to be considerably less pronounced at low deposition rates (~100 Å/min), probably because high deposition rates, like argon pressures, tend to limit the adatom surface mobility. Voided structures were suppressed at high pressures in hollow cathodes when

shields were used to limit both the side flux and the deposition rate.

At higher T/T_m (0.1-0.3) self-diffusion becomes appreciable, and coatings consist of a dense array of fibrous grains separated by more nearly conventional grain boundaries, probably due to the occurrence of a sintering type coalescence during growth. Such coatings yield high lateral strengths.

Above T/T_m~0.3-0.5 surface mobility is even greater and grain boundary migration and recrystallization are possible.[3,27] Columnar grains extending through the entire coating thickness and separated by true grain boundaries develop, possibly by surface recrystallization during growth. Argon pressure has reduced influence at these T/T_m's because of decreased surface adsorption.[28] Surfaces tend to be faceted in T/T_m range 0.5–0.75. Greater tendency for developing faceted surfaces in hollow cathode at moderate T/T_m is believed to be due to relatively low energy (30-50 eV) ion bombardment etching[8] and oblique flux of coating atoms. At very high T/T_m (~0.75) equilibrium surface structure apparently consists of relatively flat grain tops with grooved grain boundaries in both apparatuses.

Coating structure dependence on T/T_m at elevated argon pressure is similar to that described by M & D with two exceptions : (1) zone 2 columnar grains tended to be faceted, and (2) zone 3 equiaxed grains were generally not observed. At low argon pressure sputtered coatings yielded a broad zone 1-zone 2 transition region of densely packed fibrous grains not specifically described by M & D, although they do note that zone 1 grain outlines often were difficult to identify. Failure to observe equiaxed grains in the pure metals in this work was probably due to fact that deposition rates were lower (10–50 times) and that coatings were not as thick (2.5 μ) as those studied by M & D (250-2000 μ). Copper coating deposited at rates of 10 000-20 000 Å/min and high T/T_m consisted of large equiaxed grains which appear to have formed during deposition by a concurrent recrystallization process. Lower Cu deposition rates (1000-2000 Å/min) yielded columnar structures. A similar deposition rate dependence on the occurrence of room temperature after-deposition recrystallization of Cu has been reported by Patten et al.[9] High-temperature (recrystallized) equiaxed grains of M & D should not be confused with the fine-grained growth type formed by bias sputtering,[13] electroplating,[29] and CVD.[30]

Structural similarity scaling with T/T_m was not observed for all materials. Although each basic structural region was observed in most cases, transition points varied, possibly because of alloy influences and the fact that surface mobilities, heats of condensation, and vapor pressures do not vary linearly with melting point. Departures were greatest for low melting point materials, probably because the adatom kinetic energy and heat of condensation made low values of T/T_m on the condensate surface difficult to achieve for such

materials. (The M & D work was limited to the melting point range 1453-3410°C.)

ACKNOWLEDGMENT

[1]A. van der Drift, Philips Res. Rep. 22, 267 (1967).
[2]B. A. Movchan and A. V. Demshishin, Fiz. Met. Metalloved. 28, 653 (1969).
[3]J. V. Sanders, *Chemisorption and Reactions on Metallic Films*, edited by J. R. Anderson (Academic, New York, 1971), Vol. 1, p. 1.
[4]A. C. Raghuram and R. F. Bunshah, J. Vac. Sci. Technol. 9, 1389 (1972).
[5]R. F. Bunshah and R. S. Juntz, Metall. Trans. 4, 21 (1973).
[6]N. F. Kane and R. F. Bunshah, *Proceedings Fourth International Conference on* Vacuum *Metallurgy* (Iron and Steel Institute, Tokyo, 1973).
[7]Kurt Kennedy, *Transactions of the International* Vacuum *Metallurgy* Conference (American Vacuum Society, New York, 1968), p. 195.
[8]J. W. Patten and E. D. McClanahan, J. Appl. Phys. 43, 4811 (1972).
[9]J. W. Patten, E. D. McClanahan, and J. W. Johnston, J. Appl. Phys. 42, 4371 (1971).
[10]S. D. Dahlgren, E. D. McClanahan, J. W. Johnston, and A. G. Graybeal, J. Vac. Sci. Technol. 7, 398 (1970).
[11]S. D. Dahlgren and M. D. Merz, Metall. Trans. 2, 1753 (1971).
[12]R. D. Bland, J. K. Maurian and S. F. Duliere, Sandia **Laboratories** Development Report No. SC-DR-72-0922, **1972.**
[13]D. M. Mattox and G. J. Kominiak, J. Vac. Sci. Technol. 9, **528 (1972).**
[14]R. F. Bunshah and R. S. Juntz, J. Vac. Sci. Technol. 9, 1404 (1972).
[15]K. L. Chopra, *Thin Film* Phenomena (McGraw-Hill, New York, 1969), **p.** 220.
[16]P. K. Dutta and H. Wilman, J. Phys. D 3, 8.39 (1970).
[17]R. Oshima and Y. Nakamura, Jap. J. **Appl.** lPhys. 8, 844 (1969).
[18]R. Oshima, **Jap. J. Appl.** Phys. **11,** 780 (1972).
S. Kogan and A. **L. Seryugin, Fiz.** Met. Metallowed. **28. No. 4.** 49 (1969).
[20]F. M. d'Heurle Trans. Met. Soc. AIME 236, 321 (1966).
[21]E. Bauer. ngle *Crystal* Films, edited by M. H. Francombe and H. Sato (Pergamon, Oxford, 1964), p. 43.
[22]J. van de Waterbeemd, Philips Res. Rep. 21, 27 (1966).
[23]J. van de Waterbeemd and G. W. van Oosterhout, Philips Res. Ren. 22, 375 (1967).
[24]A. I. Shaldervan and N. G. Nakhodkin, Sov. Phys.-Solid State 11, 277.3 (1970).
[25]A. I. Shaldervan and N. G. Nakhodkin. Sov. Phvs.-Solid State 12, 1748 (1971).
[26]N. G. Nakhodkin and A. I. Shaldervan, Sov. Phys.-Solid State 13, 1627 (1972).
[27]P. G. Shewmon, Transformations *in Metals* (McGraw-Hill, New York, 1969), Chap. 3.
[28]H. F. Winters and E. Kay, J. Appl. Phys. 38, 3928 (1967).
[29]V. A. Lamb, *Techniques of Metals Research*, edited by R. F. Bunshah (Interscience, New York, 1968), Vol. 1, Pt. 3, p. 1311.
[30]R. A. Holzl, *Techniques of Metals Research*, edited by R. G. Bunshah (Interscience, New York, 1968), Vol. 1, Pt. 3, p. 1377.